This document is downloaded from DR-NTU (https://dr.ntu.edu.sg)
Nanyang Technological University, Singapore.

Barrier properties of thin Au/Ni–P under bump metallization for Sn–3.5Ag solder

Kumar, Aditya; He, Min; Chen, Zhong

2004

Kumar, A., He, M., & Chen, Z. (2005). Barrier properties of thin Au/Ni–P under bump metallization for Sn–3.5Ag solder. Surface and Coatings Technology, 198(1-3), 283-286.

https://hdl.handle.net/10356/95228

https://doi.org/10.1016/j.surfcoat.2004.10.085

© 2004 Elsevier B.V. This is the author created version of a work that has been peer reviewed and accepted for publication by Surface and Coatings Technology, Elsevier B.V. It incorporates referee’ s comments but changes resulting from the publishing process, such as copyediting, structural formatting, may not be reflected in this document. The published version is available at: [http://dx.doi.org/10.1016/j.surfcoat.2004.10.085].

Downloaded on 23 Aug 2022 18:19:33 SGT

Barrier properties of thin Au/Ni–P under bump metallization for Sn–3.5Ag solder

Aditya Kumar*, Min He, Zhong Chen

School of Materials Engineering Nanyang Technological University Singapore 639798, Singapore

** Corresponding author: Fax: +65 67909081. E-mail address: aditya@pmail.ntu.edu.sg (A. Kumar).*

Abstract

Electroless Ni–P with a thin layer of immersion gold has been considered as a promising under bump metallization (UBM) for low-cost flip–chip technology. However, the presence of P in electroless Ni–P causes complicated interfacial reactions, which affect the reliability of solder joint. In this work, barrier properties of thin Au/Ni–P UBM between Cu substrate and Sn–3.5Ag solder were investigated during annealing at 160, 180, and 200 °C in terms of IMC formation. Multilayer Sn–3.5Ag/Au/Ni–P/Cu sample was prepared by electroless chemical plating and solder reflow for the investigation. Annealing results showed that electroless Ni–P acts as a good barrier for Sn diffusion at 160 and 180 °C. However, it fails to protect the Cu substrate from reacting with Sn at 200 °C. The reason is that the electroless Ni–P layer starts converting into a ternary Ni–Sn–P layer at 200 °C. Complete conversion of the Ni–P layer into Ni–Sn–P, results in the formation of two Cu–Sn intermetallics, Cu_6Sn_5 and Cu_3Sn, at the Ni–Sn–P/Cu interface and the formation of $(Ni_xCu_{1-x})_6Sn_5$ intermetallic at the Ni_3Sn_4/Ni–Sn–P interface.

Keywords: Electroless Ni–P; Diffusion barrier; Interfacial reactions; Solder; Intermetallics

1. Introduction

Under bump metallization (UBM) is an essential part of low-cost solder flip–chip technology. The main functions of UBM are to provide an excellent solderable surface and to act as a diffusion barrier to protect the underlying copper from reacting with the solder. In the absence of effective UBM, the solder reacts with copper and forms intermetallic compounds (IMC) rapidly. Formation of a thin layer of IMC during soldering is desirable to achieve good metallurgical bond. However, excess growth of these IMC affects the mechanical reliability of the joint, which is a generic reliability problem in flip–chip solder joints [1–3]. This IMC growth is influenced by operating temperature of the device, which is currently in the range of −40 to 150 °C [4]. As the trend of miniaturization continues, the increase in operating temperature will speed up the IMC growth further.

Pb-containing solders are the most suitable materials for flip–chip interconnects. However, due to environmental concern on Pb, electronic industry has been replacing the Pb-containing solders with Pb-free solders. Pb-free solders are basically tin rich alloys constituting one or two more elements such as Ag, Cu, In, Sb, and Bi. These high-Sn-content solders react more rapidly with Cu UBM, forming a thick layer of Cu–Sn IMC. IMC growth weakens the solder joints as IMC are very brittle in nature and can act as an initiation site for the microcracks [5].

The IMC growth has been found to be minimized in the case of Ni UBM, as the reaction between Ni and Sn is much slower than between Cu and Sn [6]. Further, electroless Ni–P has been considered as a promising UBM due to its many advantages such as excellent selective deposition, good corrosion resistivity, strong adhesion, easy processing, and low cost as compared to thin-film vacuum processes [7–8]. However, relatively few studies have been done on the interfacial reactions between Ni–P and lead-free solders [1– 3,9–11]. It is well known that, during soldering, thin P-rich Ni–P layer forms in between the Ni–Sn IMC and original Ni–P layers due to solder-assisted crystallization of electroless Ni–P. Jang et al. [1] and Hung et al. [9] found that Ni_3Sn_4 formed at the Ni–P/solder interface during the interfacial reaction with a thin layer of

Ni_3P underneath the Ni_3Sn_4. However, Alam et al. [10] and Inaba et al. [11] reported additional Ni–Sn IMC and Ni–P compounds at the solder/Ni–P interface. All these investigations were carried out at liquid-state reflow temperatures. In the present work, we investigated the barrier properties of Au/Ni–P UBM for the Sn–3.5Ag solder on the Cu metallization at solid-state annealing temperatures. Growth mechanism of various IMC formed during the interfacial reactions were also discussed in detail.

2. Experimental procedures

For the investigation, a sample having multilayer structure, Sn–3.5Ag/Au/Ni–P/Cu, shown in Fig. 1, was prepared. Initial stage of sample preparation involved deposition of electroless Ni–P on a surface-cleaned commercial copper substrate of around 3 mm thick. A very thin layer (~200 Å) of noncyanide immersion gold was then deposited on the Ni–P surface to protect the surface from oxidation. A thick layer of Sn–3.5Ag solder was then coated on the substrate by placing the solder wires on the substrate and then reflowing them at 245 °C for 60 s. No-clean flux was applied on the substrates before placing the Sn–3.5Ag wires. Finally, the substrates were cut into small samples of size 5 × 5 mm with the help of a diamond saw.

The as-prepared sample was annealed in an oven at 160, 180, and 200 °C for various durations from 48 to 400 h. After annealing, the sample was removed from the oven and cooled in air. Scanning electron microscope (SEM) was used for microstructural analysis of the cross-sectioned samples. For SEM observation, the samples were cold-mounted in epoxy and polished down to 1-μm finish. After polishing, solder etching was carried out to reveal the microstructure in cross-section. Etching was done with 4% (by volume) hydrochloric acid for a few seconds. Energy dispersive X-ray (EDX) spectroscopy was performed in the JEOL JSM-5410LV SEM to analyze the chemical composition of electroless Ni–P and the IMC.

3. Results

Fig. 2a is the micrograph of Sn–3.5Ag/Ni–P/Cu interfaces in the as-prepared sample, showing the formation of needle-type and chunky-type IMC at the Sn–3.5Ag/Ni–P

interface during the reflow. A dark thin layer having small columnar-shaped voids also formed in the Ni–P layer underneath the IMC (Fig. 2b). Average thickness of solder, Ni–P, and IMC layers were measured to be around 210, 6.5, and 2.5 μm, respectively. During the reflow, Au layer completely dissolved in the solder, as EDX analysis did not show the presence of Au or Au–Sn IMC at the interface. Quantitative EDX analysis showed that IMC has 43.7 at.% Ni and 56.3 at.% Sn, Ni–P layer has 89.3 at.% Ni and 10.7 at.% P, and dark thin layer has 79.1 at.% Ni and 20.9 at.% P. Thus, needle and chunky-type Ni_3Sn_4 formed at the Sn–3.5Ag/Ni–P interface with a P-rich Ni–P layer underneath the Ni_3Sn_4 during the reflow. These results are in agreement with the previous interfacial studies between electroless Ni–P and Sn–3.5Ag solder [1–3,9–11].

During annealing, it was observed that the size and number of columnar-shaped voids in the P-rich layer increased with the duration and temperature of annealing. Fig. 3a and b, respectively, are the micrographs of Sn–3.5Ag/Ni–P interface in the samples annealed for 400 h at 160 °C and 180 °C, showing the formation of a large number of columnar shaped voids in the P-rich layer. Despite the formation of voids, electroless Ni–P was very stable at 160 and 180 °C for up to 400 h annealing. However, at 200 °C for 48 h annealing, most part of the Ni–P layer had big columnar-shaped voids and the part close to Ni_3Sn_4 had traces of Sn, as shown in Fig. 4a. The elemental composition of this Sn-containing Ni–P layer was 54.5 at.% Ni, 28.9 at.% Sn, and 16.6 at.% P. It was also observed that Ni–P, just below the Sn-containing Ni–P layer, converted into P-rich Ni–P. The P content of this P-rich Ni–P layer was around 19.8 at.%. This P content and the presence of voids in the P-rich Ni–P layer support the previous reports that P-rich layer is a mixture of Ni–P compounds [3,11].

Fig. 4b is a micrograph showing Sn–3.5Ag/Ni–P interface in the sample annealed at 200 °C for 400 h. The entire Ni–P layer was converted into a ternary Ni–Sn–P layer during prolonged annealing at 200 °C. Two types of Cu–Sn IMC, Cu_6Sn_5 and Cu_3Sn, were found at the Ni–Sn–P/Cu interface. The Cu_3Sn IMC was found to be close to Cu surface, understood to be due to the large availability of Cu from the Cu substrate. High Cu content was observed in Ni_3Sn_4 layer at the Ni_3Sn_4/Ni–Sn–P interface. The elemental composition of this Ni–Cu–Sn layer was 26.2 at.% Ni, 29.4 at.% Cu, and 44.4 at.% Sn,

indicating the formation of $(Ni_xCu_{1-x})_6Sn_5$ phase. Thus, after conversion of Ni–P into Ni–Sn–P, the Sn reached to the Cu substrate and formed Cu–Sn IMC at the Ni–Sn–P/Cu interface. The Ni–Sn–P layer could not be able to hinder the Cu to diffuse out from the substrate. As a result, Cu diffused through the Ni–Sn–P layer and formed $(Ni_xCu_{1-x})_6Sn_5$ intermetallic at the Ni_3Sn_4/Ni–Sn–P after reacting with Ni_3Sn_4.

4. Discussion

In this work, annealing was carried out up to 200 °C, well below 221 °C, the melting temperature of Sn–3.5Ag solder. Reflow process causing the formation of Ni–Sn–P layer has already been reported, whereas complete conversion of the Ni–P layer into Ni–Sn–P during solid-state annealing was observed for the first time in this work. Recently, Matsuki et al. [12] reported the presence of a thin layer of Ni_2SnP in between Ni–Sn IMC and P-rich Ni–P layers during the reflow, while Hwang et al. [13] reported Ni_3SnP IMC. Thus, it can be concluded that the formation of Ni–Sn–P IMC between Ni_3Sn_4 and P-rich Ni–P layers is due to the reaction between Sn and Ni–P, but no unique composition has been established. The composition of the Ni–Sn–P layer observed in this investigation suggests either the formation of solid solution phase or formation of a mixture of different phases. Moreover, Furuseth and Fjellvag [14] also reported the formation of Ni–Sn–P solid-solution phase, having the composition in the range of $Ni_{1+m}Sn_{1-x}P_x$ ($0.00 \leq m \leq 0.65, 0.00 \leq x \leq 0.32$), which is similar to that observed in this investigation. Thus, it can be concluded that Sn reacts with P-rich Ni–P layer and forms either Ni–Sn–P solid-solution phase or mixture of different phases during high-temperature annealing at 200 °C.

Growth mechanisms of IMC in the Sn–3.5Ag/Ni–P/Cu solder joint are to be understood well as they influence the reliability. Small Kirkendall voids were observed in P-rich Ni–P layer formed during the reflow (Fig. 2b). The size of the voids as well as their number increased with temperature and duration of annealing (Fig. 3a,b). The formation and growth of Kirkendall voids indicate that, during annealing, Ni diffuses from original Ni–P to Ni_3Sn_4/P-rich Ni–P interface, resulting in a counter diffusion of vacancies. These vacancies accumulate and form voids in the P-rich Ni–P layer [15]. The

depletion of Ni from the original Ni–P layer assists the original Ni–P layer to crystallize into Ni–P compounds and increases the P-rich Ni–P layer thickness.

It was also observed that prolonged high-temperature annealing resulted in large Ni_3Sn_4 growth, thereby causing large depletion of Ni from original Ni–P layer. After original Ni–P layer was fully consumed, the Sn from the solder started reacting with the P-rich Ni–P layer and formed Ni–Sn–P (Fig. 4a). After the complete conversion of the P-rich Ni–P layer into Ni–Sn–P, the Sn coming from the solder started reacting with Cu and formed Cu_6Sn_5 and Cu_3Sn at the Ni–Sn–P/Cu interface (Fig. 4b). Simultaneously, Cu started diffusing out from the substrate and formed $(Ni_xCu_{1-x})_6Sn_5$ intermetallic at the Ni_3Sn_4/Ni–Sn–P interface due to the reaction with Ni_3Sn_4. A schematic illustration of IMC growth in the Sn–3.5Ag/Ni–P/Cu solder joint is shown in Fig. 5. The complete growth mechanism can be divided into three stages. In stage I, a thin layer of P-rich Ni–P is formed underneath the Ni_3Sn_4, whose thickness increases with annealing time. When the supply of Ni from the original Ni–P is not sufficient, the P-rich Ni–P layer starts reacting with Sn and converts into the Ni–Sn–P layer (stage II). In the final stage, after conversion of the entire Ni–P layer into Ni–Sn–P, the Sn reaches to Cu substrate and forms Cu_3Sn and Cu_6Sn_5 IMC. During the same time, Cu also diffuses out to Ni_3Sn_4 layer and forms $(Ni_xCu_{1-x})_6Sn_5$ at the Ni_3Sn_4/Ni–Sn–P interface.

5. Conclusions

In summary, barrier properties of Au/Ni–P UBM for Sn–3.5Ag solder on Cu metallization was studied at 160, 180, and 200 °C. It was found that electroless Ni–P acts as a good diffusion barrier for the Sn–3.5Ag solder during the reflow at 245 °C for 60 s as well as during the prolonged solid-state annealing at 160 and 180 °C. However, it fails to protect the copper metallization from Sn at 200 °C. Electroless Ni–P layer started converting into Ni–Sn–P layer at 200 °C even during the short period of annealing (48 h). Prolonged annealing at 200 °C resulted in the complete conversion of Ni–P layer into Ni–Sn–P and then in the formation of $(Ni_xCu_{1-x})_6Sn_5$ and Cu–Sn IMC at the Ni_3Sn_4/Ni–Sn–P and Ni–Sn–P/Cu interfaces, respectively. Conversion of electroless Ni–P layer into Ni–

Sn–P during annealing at 200 °C proved that Ni–P is not a good diffusion barrier to Sn–3.5Ag solder for high-temperature applications.

References

[1] J.W. Jang, P.G. Kim, K.N. Tu, D.R. Frear, P. Thompson, J. Appl. Phys. 85 (1999) 8456.

[2] J.W. Jang, D.R. Frear, T.Y. Lee, K.N. Tu, J. Appl. Phys. 88 (2000) 6359.

[3] M.O. Alam, Y.C. Chan, K.N. Tu, J. Appl. Phys. 94 (2003) 4108.

[4] International Technology Roadmap for Semiconductors (Assembly and Packaging), Semiconductor Industry Association, San Jose, 2001.

[5] L.E. Felton, A.D. Selsley, P.J. Ficalora, Appl. Phys. Lett. 54 (1989) 2074.

[6] K.N. Tu, K. Zeng, Mater. Sci. Eng., R 34 (2001) 1.

[7] C.Y. Lee, K.L. Lin, Thin Solid Films 249 (1994) 201.

[8] J.G. Strandjord, S. Popelar, C. Jauernig, Microelectron. Reliab. 42 (2002) 265.

[9] K.C. Hung, Y.C. Chan, C.W. Tang, H.C. Ong, J. Mater. Res. 15 (2000) 2534.

[10] M.O. Alam, Y.C. Chan, K.C. Hung, J. Electron. Mater. 31 (2002) 1117.

[11] M. Inaba, K. Yamakawa, N. Iwase, IEEE Trans. CHMT 13 (1990) 119.

[12] H. Matsuki, H. Ibuka, H. Saka, Sci. Technol. Adv. Mater. 3 (2002) 261.

[13] C.-W. Hwang, K. Suganuma, M. Kiso, S. Hashimoto, J. Mater. Res. 18 (2003) 2540.

[14] S. Furuseth, H. Fjellvag, Acta Chem. Scand. 48 (1994) 134.

[15] M. He, Z. Chen, G. Qi, Acta Mater. 52 (2004) 2047.

List of Figures

Fig. 1 Schematic diagram of solder joint showing multilayer structure, Sn–3.5Ag/Au/Ni–P/Cu.

Fig. 2 SEM image of as-prepared sample (a) Sn–3.5Ag/Ni–P/Cu interfaces; (b) magnified view of Sn–3.5Ag/Ni–P interface shown in panel (a) by a rectangle.

Fig. 3 SEM image of the Sn–3.5Ag/Ni–P/Cu interfaces in the sample annealed at different temperatures for 400 h: (a) 160 and (b) 180 °C.

Fig. 4 SEM image of Sn–3.5Ag/Ni–P/Cu interfaces in the sample annealed at 200 °C for (a) 48 and (b) 400 h.

Fig. 5 Schematic illustration for IMC growth in the Sn–3.5Ag/Ni–P/Cu multilayer structure, showing different stages of growth mechanism: (I) formation of thin P-rich Ni–P layer in between Ni_3Sn_4 and original Ni–P layer during soldering; (II) conversion of P-rich Ni–P layer into Ni–Sn–P layer due to the reaction between Sn and P-rich Ni–P; (III) formation of Cu–Sn and $(Ni_xCu_{1-x})_6Sn_5$ IMC due to the reaction between Cu and Sn and between Cu and Ni_3Sn_4, respectively.

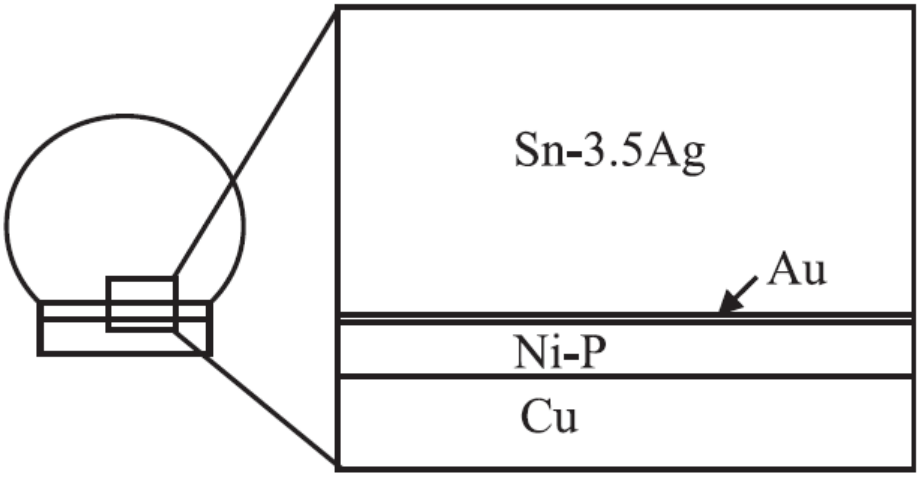

Fig. 1

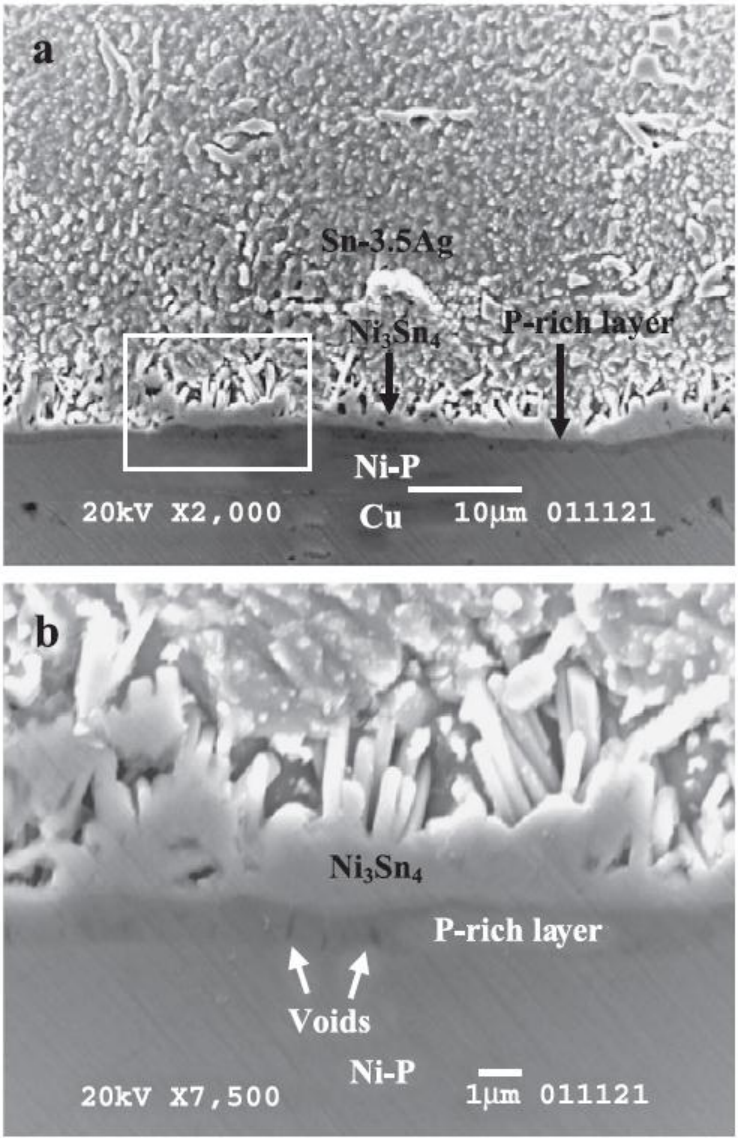
a
Sn-3.5Ag
Ni3Sn4
P-rich layer
Ni-P
20kV X2,000
Cu
10μm 011121
b
Ni3Sn4
P-rich layer
Voids
Ni-P
20kV X7,500
1μm 011121

Fig. 2

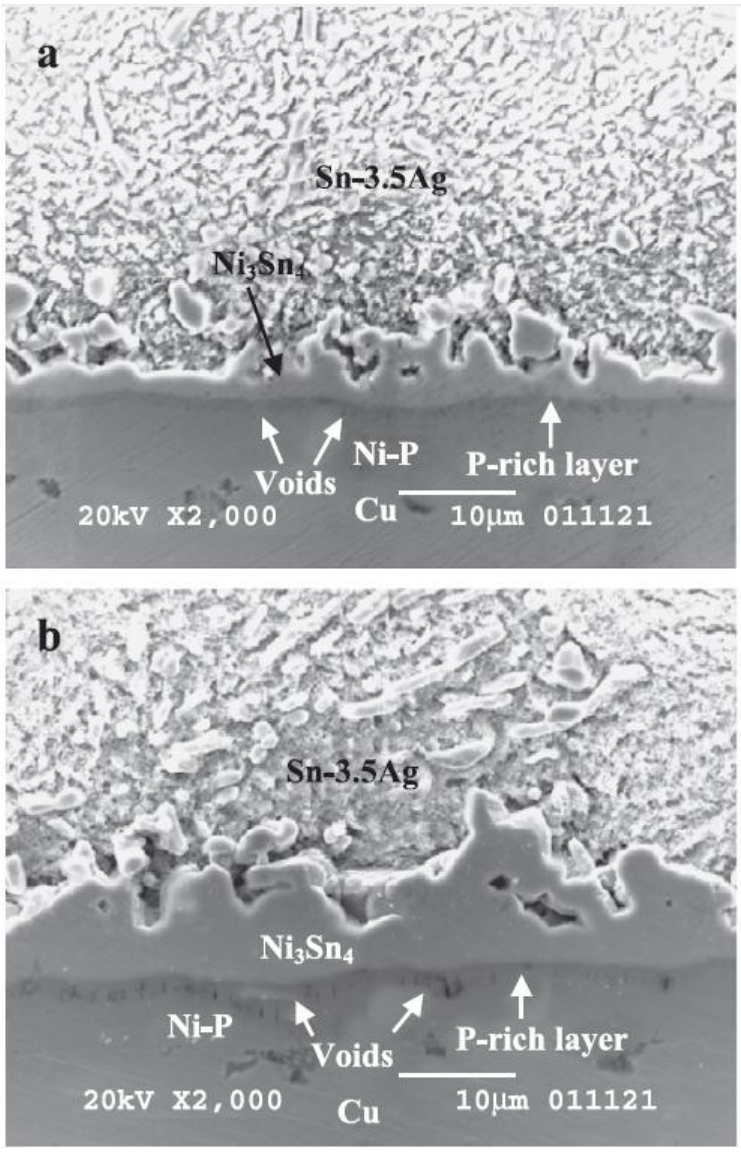
a
Sn-3.5Ag
Ni3Sn4
Voids
Ni-P
P-rich layer
20kV X2,000
Cu
10μm 011121
b
Sn-3.5Ag
Ni3Sn4
Ni-P
Voids
P-rich layer
20kV X2,000
Cu
10μm 011121

Fig. 3

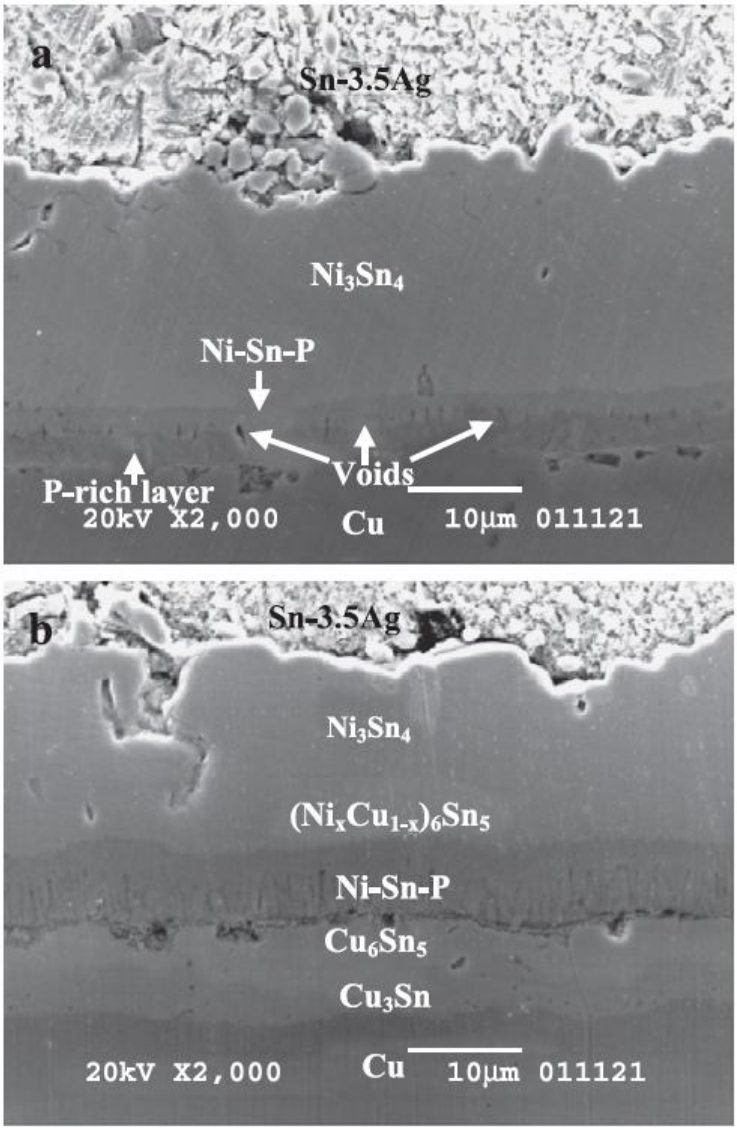
a
Sn-3.5Ag
Ni3Sn4
Ni-Sn-P
Voids
P-rich layer
20kV X2,000
Cu
10μm 011121
b
Sn-3.5Ag
Ni3Sn4
(NixCu1-x)6Sn5
Ni-Sn-P
Cu6Sn5
Cu3Sn
20kV X2,000
Cu
10μm 011121

Fig. 4

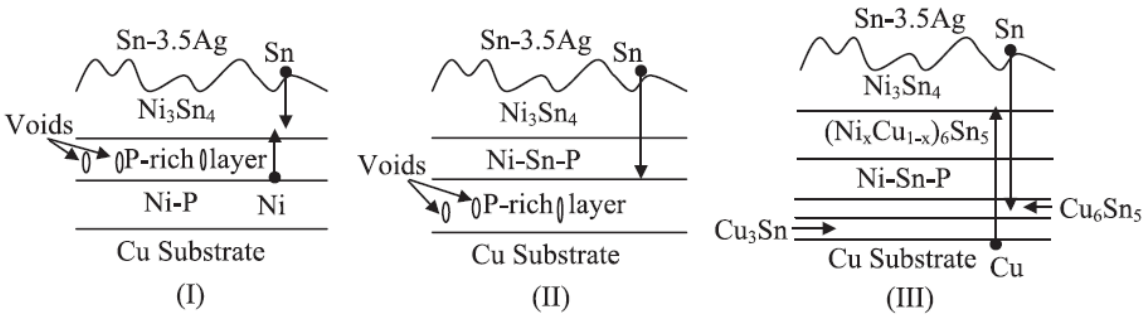
Sn-3.5Ag
Sn
Ni3Sn4
Voids
P-rich layer
Ni-P
Ni
Cu Substrate
(I)
Sn-3.5Ag
Sn
Ni3Sn4
Voids
Ni-Sn-P
P-rich layer
Cu Substrate
(II)
Sn-3.5Ag
Sn
Ni3Sn4
(NixCu1-x)6Sn5
Ni-Sn-P
Cu6Sn5
Cu3Sn
Cu Substrate
Cu
(III)

Fig. 5